Single-Molecule Imaging Reveals Aβ42:Aβ40 Ratio-Dependent Oligomer Growth on Neuronal Processes

Robin D. Johnson,[††‡*] Joseph A. Schauerte,[†] Chun-Chieh Chang,[†] Kathleen C. Wisser,[†] John Christian Althaus,[§] Cynthia J. L. Carruthers,[§] Michael A. Sutton,[§¶] Duncan G. Steel,[†‖**] and Ari Gafni[†††]

[†]Department of Biophysics, [‡]Medical Scientist Training Program, [§]Molecular and Behavioral Neuroscience Institute, [¶]Department of Molecular and Integrative Physiology, [‖]Department of Physics, [**]Department of Electrical Engineering and Computer Science, and [††]Department of Biochemistry, University of Michigan, Ann Arbor, Michigan

ABSTRACT　Soluble oligomers of the amyloid-β peptide have been implicated as proximal neurotoxins in Alzheimer's disease. However, the identity of the neurotoxic aggregate(s) and the mechanisms by which these species induce neuronal dysfunction remain uncertain. Physiologically relevant experimentation is hindered by the low endogenous concentrations of the peptide, the metastability of Aβ oligomers, and the wide range of observed interactions between Aβ and biological membranes. Single-molecule microscopy represents one avenue for overcoming these challenges. Using this technique, we find that Aβ binds to primary rat hippocampal neurons at physiological concentrations. Although amyloid-β(1–40) as well as amyloid-β(1–42) initially form larger oligomers on neurites than on glass slides, a 1:1 mix of the two peptides result in smaller neurite-bound oligomers than those detected on-slide or for either peptide alone. With 1 nM peptide in solution, Aβ40 oligomers do not grow over the course of 48 h, Aβ42 oligomers grow slightly, and oligomers of a 1:1 mix grow substantially. Evidently, small Aβ oligomers are capable of binding to neurons at physiological concentrations and grow at rates dependent on local Aβ42:Aβ40 ratios. These results are intriguing in light of the increased Aβ42:Aβ40 ratios shown to correlate with familial Alzheimer's disease mutations.

INTRODUCTION

Alzheimer's disease (AD), the sixth leading cause of death in the United States, is characterized by the development of extracellular plaques composed of fibrils of amyloid-β peptide (1). In recent years, emerging evidence has caused the amyloid cascade hypothesis (which implicates plaques in AD neurotoxicity) to be largely supplanted by an amyloid oligomer hypothesis (2). This concept presents small amyloid-β oligomers as the synaptotoxic molecular structures that lead to AD. Amyloid-β is a 39-to-43 residue peptide produced by β- and γ-secretase cleavage of an integral membrane protein, amyloid-precursor peptide (3). Many of the ~10% of AD cases that are genetic in nature (familial Alzheimer's disease, or FAD) are correlated with mutations in presenilin, the catalytic subunit of γ-secretase. Such mutations frequently increase the ratio of Aβ42/Aβ40, which may contribute strongly to AD development in these patients (3,4).

Aβ is present in both normal and AD human brain tissue at subnanomolar to low nanomolar concentrations (5,6). At these low concentrations, the oligomeric state of the peptide is thought to be in a constant state of flux, with small aggregates (monomers to hexamers) interconverting in a dynamic equilibrium (7–9). These factors complicate attempts to use existing data to draw conclusions about actual conformational and stoichiometric states of Aβ in the human brain.

Numerous specific components of the lipid bilayer have been implicated as Aβ-binding sites through which toxicity might be mediated. These include externalized phosphatidylserines (10,11), GM1 ganglioside containing micro- or nanodomains (12,13), and regions with increased cholesterol content (14). However, substantial evidence has also been put forth for protein receptors as probable Aβ-binding sites (15), including α-7 nicotinic acetylcholine receptors (α7nAchRs) (16), the cellular prion protein (PrP^C) (17), metabotrobic glutamate receptor 5 (mGluR5) (18), and EphB2 receptors (19). Most of these integral membrane protein receptors for Aβ have been proposed in an effort to explain the peptide's well-documented effects on synaptic plasticity. Although they provide interesting directions for future study, these experiments have generally been performed in model mouse systems, at higher than physiological Aβ concentrations, or using Aβ oligomers prepared in vitro.

Several distinct subfibrillar Aβ aggregates isolated in laboratory settings have been characterized and may contribute to AD neurotoxicity. These include low-n oligomers such as sodium dodecyl sulfate (SDS)-stable dimers, trimers, and tetramers, ADDLs (amyloid-derived diffusible ligands), the Aβ*56 dodecameric oligomer, AβOs, ASPDs (SDS-stable amylospheroids), and APFs (annular protofibrils) (20). The role of membrane interactions in the formation of these toxic Aβ oligomers is a subject of particularly strong debate. A number of groups have found that preaggregated Aβ induces greater toxicity than monomeric or fibrillar Aβ, implying that oligomers formed in solution without contact with biological membranes must be capable

CrossMark

of interacting with cell membrane moieties (21,22). However, treatment of biological membranes with unaggregated Aβ is also associated with toxicity, more specifically with formation of cation-selective pores as evidenced by stepwise membrane conductance changes (23,24).

The wide variation in observed binding sites and proposed oligomer structure reflects fundamental uncertainties in the field regarding how Aβ oligomers form, interact with membranes, and behave following binding. Recently, Zhang and associates used surface pressure measurements to determine the relative abilities of monomeric Aβ, ADDLs, and protofibrillar Aβ to insert into planar membranes (25). Monomers of the peptide inserted into the membrane more rapidly than oligomers of either type and oligomerized, following binding, in a process distinct from oligomerization in solution. Zhang et al. (25) proposed that intramembrane and extramembrane oligomerization may produce two separate pools of Aβ whose toxicities are mediated by completely distinct mechanisms. Oligomers formed in the membrane may directly disrupt membrane integrity by transient pore formation, allowing toxic calcium influx. At the same time, oligomers formed in solution may, as previously discussed, interact with specific cellular receptors, altering their function and resulting in toxicity. Of importance, at physiological concentrations, any toxicity induced by binding of monomeric peptide and subsequent formation of oligomers likely occurs gradually. For example, Shankar and colleagues (26) demonstrated significant immediate drops in longterm potentiation with application of dimers isolated from human brain at subnanomolar levels. However, little decrease in long-term potentiation was observed with application of synthetic, initially monomeric Aβ40 at concentrations below 50–100 nM. Our own recent work showed that application of 50 nM monomeric Aβ40 induces only very subtle leakage of calcium into SH-SY5Y cells, though onmembrane oligomer formation occurs within minutes (27). However, the low concentration regime still represents an important area of study. Understanding the mechanics of amyloid-β's interactions with membranes at physiological concentrations, before the induction of grossly observable toxicity, may be necessary for the development of targeted neuroprotective therapy.

Our group has recently used single-molecule microscopy to study the size distributions of Aβ aggregates generated at physiological concentrations in solution (9), on planar model membranes (28), and on living SH-SY5Y neuroblastoma cells (27). Single-molecule microscopy provides several advantages for the study of this system. Experiments can be performed at low concentrations to more closely simulate peptide concentrations in the brain. Dynamics of rapidly shifting oligomer populations and the motion of individual particles can be easily monitored over time. Single oligomers that might be lost in an ensemble measurement can be resolved and potentially associated with specific binding locations. These properties combine to make single-molecule techniques uniquely well suited for studies of Aβ-membrane interactions.

Here, we show that single-molecule microscopy of HL647Aβ is feasible on the processes of primary hippocampal neurons in culture. We show that Aβ binds to neurites at physiological peptide concentrations within minutes and that these early oligomers do not preferentially bind to synapses. Interestingly, the binding and evolution of oligomers on neurites is strongly affected by the stoichiometry of Aβ40 and Aβ42 peptides. Initial neurite-bound HL647Aβ40 and HL647Aβ42 oligomers are shown to be larger than those bound nonspecifically to coverslips, but undergo little growth over the course of additional 48-h incubation. A 1:1 mix of the two peptides, however, initially appears on neurites as very small oligomers, but these grow substantially over the next 2 days. Our results imply that localized increases in the Aβ42:Aβ40 ratio, independently of changes in overall Aβ concentration, significantly alters the kinetics of on-membrane oligomer growth.

METHODS

Peptide preparation

Synthetic unlabeled amyloid-β(1–40), N-terminally HiLyte Fluor 647-labeled amyloid-β(1–40), and (1–42) (HL647Aβ40 and 42, respectively), and HiLyte Fluor 647 hydrazide were obtained from Anaspec (Freemont, CA). Amyloid-β (Aβ) peptides were dissolved in 1% NH_4OH at 0.1 mg/mL and vortexed for 30 s to mix. Peptides were lyophilized and stored at −20°C. To prepare fresh Aβ samples, single aliquots were dissolved in 10 mM sodium phosphate buffer, pH 7.4, at 1 to 2 μM, and pipetted 5 to 8 times to mix. Freshly prepared Aβ was used within 1 h. For spin-coated sample preparation, freshly solubilized HL647Aβ40 or HL647Aβ42 was diluted to 0.5 nM in 10 mM sodium phosphate, pH 7.4, and 100 μL of this was spin-coated onto a kilned glass slide.

Primary rat hippocampal cell culture

Primary rat hippocampal neuron cultures were prepared as described (29). Cells were plated at 30,000/well on 14 mm poly-D-lysine coated glass coverslips adhered to 35 mm culture dishes (MatTek, Ashland, MA). Imaging experiments were performed between DIV 12 and DIV 18. For single molecule oligomer size measurement experiments, cells were incubated for 10 min at 37°C in HBS (HEPES-Buffered Saline: 119 mM NaCl, 5 mM KCl, 2 mM CaCl2, 2 mM MgCl2, 30 mM Glucose, 10 mM HEPES, pH 7.4) containing 1 nM HL647Aβ, washed three times in HBS, and imaged at room temperature in HBS within an hour of exposure. For time course experiments, following initial incubation with 1 nM HL647Aβ, cells were placed back in the original media containing either no Aβ or 1 nM Aβ and incubated at 37°C for the time specified. Immediately before imaging, cells were washed three times in HBS and then imaged within an hour.

Fluorescence lifetime measurements

Fluorescence lifetimes of HL647 hydrazide, HL647Aβ40, and HL647Aβ42 were assessed using the Time-Resolved Confocal Microscope ALBA System (Champaign, IL) at the University of Michigan SMART (single molecule analysis in real time) Center. Fitting the resulting decay curves

yielded fluorescence lifetimes of 1.538 ± 0.009 ns for the HL647 hydrazide free dye, 1.646 ± 0.002 ns for the HL647Aβ40, and 1.688 ± 0.004 ns for the HL647Aβ42. The slightly increased lifetimes of the dye when bound to the peptide likely reflect slight changes to the local electronic environment. As these lifetimes are not equivalent within experimental error, the HL647 hydrazide fluorescence intensity per monomer was multiplied by 1.0702, the ratio of $\tau_{HL647AB40}/\tau_{HL647}$, obtain expected intensity per HL647Aβ40 monomer. For HL647Aβ42, the correction ratio (ratio of $\tau_{HL647AB42}/\tau_{HL647}$) was 1.0974, and for experiments with a 1:1 mix of the two peptides, the average of the two ratios, 1.0838, was used to determine expected monomer intensity.

Confocal mode integrated intensity-based oligomer size determination

We recently used confocal mode fluorescence intensity to measure oligomer size on black lipid membranes (28). To measure oligomer size on living cells, we developed a protocol to correlate particles' confocal mode fluorescence intensity values with the number of Aβ monomers they contain (27). When laser power is below saturation, the fluorophore emission varies linearly with excitation power. Under these conditions, the slope of total intensity from a given volume versus the number of molecules present in the volume yields intensity per molecule. The fluorescence intensity of an oligomer can be divided by this value to yield the number of Aβ monomers present in the oligomer (assuming the quantum yields of the free dye and peptide-bound dye are the same). Single oligomer size measurements were performed here as described (27) (also see the Supporting Material). Briefly, primary cultures were imaged within 1 h of removal from incubators. Cell-bound oligomers were defined as those fluorescence spots whose maxima fell on or within 500 nm of a neurite and were boxed with a 40 pixel × 40 pixel (~1.6 μm × 1.6 μm) region of interest. Following subtraction of background fluorescence counts, the integrated fluorescence intensity of each region of interest was divided by fluorescence intensity per molecule to determine oligomer size.

RESULTS

Single HL647Aβ40 oligomers bind to primary rat hippocampal neurites

In preliminary experiments for the study of single Aβ oligomers on neurites, primary rat hippocampal cultures were exposed to 50 nM HL647Aβ40 for 10 min and imaged at single-molecule sensitivity. HL647Aβ40 bound strongly to neurites at this concentration (top left image, Fig. 1), at too high a density for detection of individual oligomers. Optimal binding densities for single-molecule detection were obtained at a concentration of 1 nM (middle left image, Fig. 1). Of note, in multiple preliminary experiments assessing calcium leakage, grossly observable changes in calcium transient frequency and spine density over an hours-to-days timescale, Aβ treatment at concentrations <10 nM produced no significant toxicity compared to controls. To ensure that starting material contained unaggregated peptide, single-molecule photobleaching experiments were performed on dry spin-coated samples of freshly prepared HL647Aβ40 and HL647Aβ42, as in our previous work with live cells (27). Over 90% of single peptide species in these samples bleached as monomers, with the vast majority of the remainder bleaching as dimers (Fig. S1 in

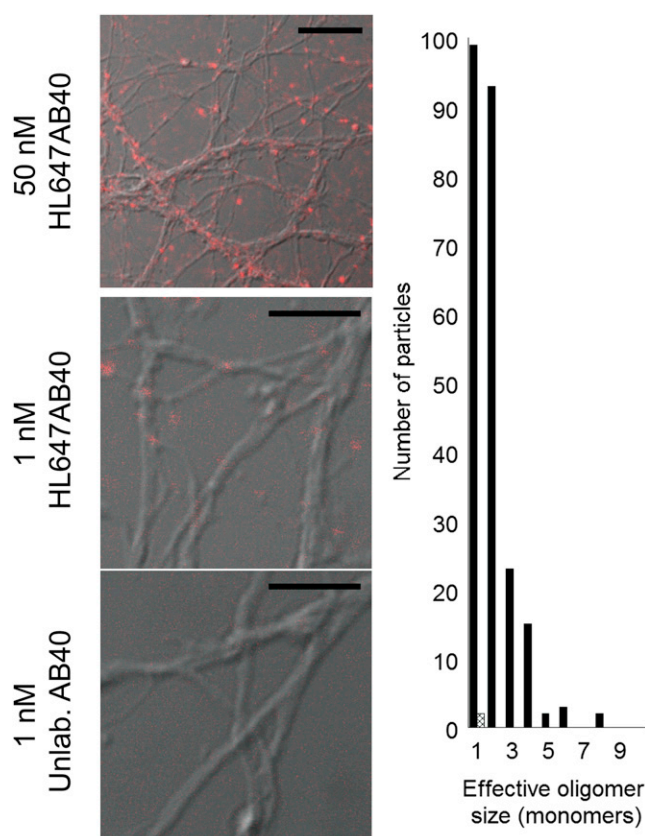FIGURE 1   Amyloid-β(1–40) binds to primary rat hippocampal neurites with high affinity. Very densely bound oligomers are visible on neurites treated for 10 min with 50 nM HL647Aβ40 (top left image, scale bar 10 μm). Single oligomers are detected on neurites treated with 1 nM HL647Aβ40 (middle image, scale bar 5 μm), but not on neurites treated with 1 nM unlabeled Aβ40 as a control (bottom image, scale bar 5 μm). Analysis of 20 frames of neurites in each 1 nM-treated sample (right plot) yielded 237 single particles in HL647Aβ40-treated neurites (black bars), but only two particles with intensity equivalent to monomers in unlabeled Aβ40-treated neurites (hatched bar).

the Supporting Material). Confocal integrated intensity oligomer size measurement was also verified by comparison with the single-molecule photobleaching method for HL647Aβ42, as was done for labeled Aβ40 in our previous work (Fig. S2) (27). Comparison of oligomer size histograms from 20 images acquired in cultures treated with unlabeled Aβ40 (bottom left image, Fig. 1) and HL647Aβ40 reveals that autofluorescence is minimal in these samples (plot at right, Fig. 1). In 20 images from the unlabeled Aβ40 sample, only two particles with brightness equivalent to monomers were detected. A total of 237 particles with fluorescence intensity ranging from monomer equivalent to octamer equivalent were detected in 20 HL647Aβ40 images. These results confirmed that primary rat hippocampal neurites treated briefly with HL647Aβ40 and HL647Aβ42 represented a suitable system for single-molecule study of Aβ oligomer membrane binding and growth.

Neurite-bound Aβ40 and Aβ42 oligomers are larger than slide-bound oligomers

Our earlier results indicate that Aβ40 binds rapidly to living cells and forms larger oligomers on the membranes of these cells than on the glass coverslips to which the cells are adhered (27). Results on neurites were consistent with this earlier observation: oligomers again bound both to slides and to cell membrane at the peptide concentrations used for the study (Fig. S3). Raw oligomer size distributions for HL647Aβ40 and HL647Aβ42 oligomers detected on neurites were significantly shifted toward larger particles, as compared to the distributions obtained for slide-bound oligomers (Mann-Whitney U-test, $p < 0.00001$ for both Aβ40 and Aβ42). On-slide HL647Aβ40 and HL647Aβ42 oligomers had an average size of 1.4 peptide subunits, whereas the average respective neurite-bound oligomer sizes were 2.2 and 1.9 peptide subunits. As seen in Fig. 2, for both Aβ40 and Aβ42 oligomers detected on-slide, monomers comprised the largest reservoir of peptide, containing 45% to 50% of the total. However, for Aβ40
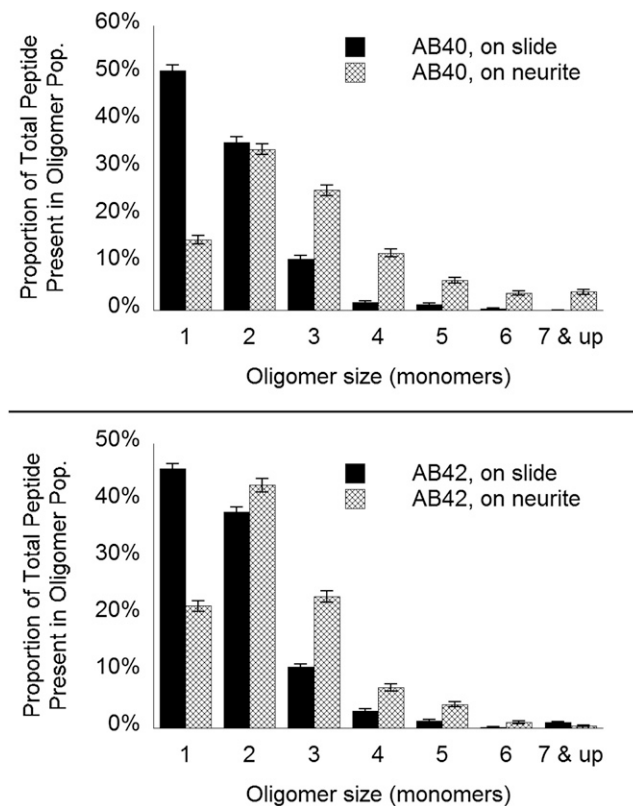

FIGURE 2 Aβ40 and Aβ42 oligomers on neurites are larger than those on slides. Distributions are shown as percentage of total peptide present within each oligomer population for HL647Aβ40 (*top*) and HL647Aβ42 (*bottom*), nonspecifically bound to slides (*black*) or bound to primary rat hippocampal neurites (*cross-hatched*). Proportions were calculated using compiled data from three separate experiments, 20 images each. Each sample contains at least 1600 peptide subunits present in a minimum of 750 particles. Error bars represent standard error of the percentage.

and Aβ42 on neurites, dimers contained the highest proportion, respectively 36% and 43% of the total peptide.

A number of groups have observed that Aβ oligomers localize to synapses (18,30,31). To determine whether the small HL647Aβ40 and HL647Aβ2 oligomers we observe on neurites bind preferentially to synapses, neurites treated with 5 nM peptide were stained for PSD-95, a postsynaptic membrane marker protein, or for Aβ (as a positive control) (Fig. S4). Although significant colocalization is observed between HL647Aβ and anti-Aβ antibody on neurites (Fig. S4), comparatively little overlap is visible between PSD-95 and HL647Aβ40 or HL647Aβ42. This indicates that small oligomers formed at physiological concentrations of HL647Aβ on neurites do not preferentially bind to synapses, at least initially. The difference between this observation and that of previous studies (18,30,31) is addressed in the Discussion. Briefly, one explanation for this result might be that Aβ binds to a pre- or postsynaptic receptor molecule that is predominantly present at the synapse only under certain conditions. Therefore, if a substantial portion of the proposed Aβ receptor population were extrasynaptic under our experimental conditions, bound Aβ might not appear to colocalize with synapses.

Depending on whether the targeted receptor is presynaptic or postsynaptic, it could be expected to be expressed at a higher density on axons than on dendrites or vice versa. In fact, surface density of certain posited Aβ receptors or target proteins has been shown to be site-specific, with mGluR5, NMDA receptors, and cellular prion protein all more strongly concentrated on dendrites or at the postsynaptic membrane than on axons (17,32,33). Measurement of the number of receptors per unit length would include both extrasynaptic and intrasynaptic populations. Therefore, we hypothesized that if a substantial portion of the Aβ receptor population were extrasynaptic, and Aβ binds to a postsynaptic receptor, Aβ would bind more densely on dendrites than on axons. To test this, we assessed bound oligomer density on neurites treated with 5 nM HL647Aβ and then stained with specific markers for axons and dendrites and binding density per unit length was measured. The values were compared to determine whether the oligomers exhibited any preference for one type of neurite over the other. HL647Aβ40 and HL647Aβ42 oligomer binding densities were respectively 20% and 40% higher on dendrites than on axons (Fig. S5).

Two groups have recently studied the motion of premade Aβ42 oligomers on live cell membranes (18,34). To study the motion of neurite-bound oligomers detected here, 10-frame xyt scans were performed on cultures treated with 1 nM HL647Aβ. Kymographs were then assembled to determine whether oligomers exhibited significant motion over the 2 min during which the scans were acquired. Oligomers were sorted into categories based on whether they exhibited significant motion. Examples of kymographs for oligomers falling in each category are shown in the Supporting
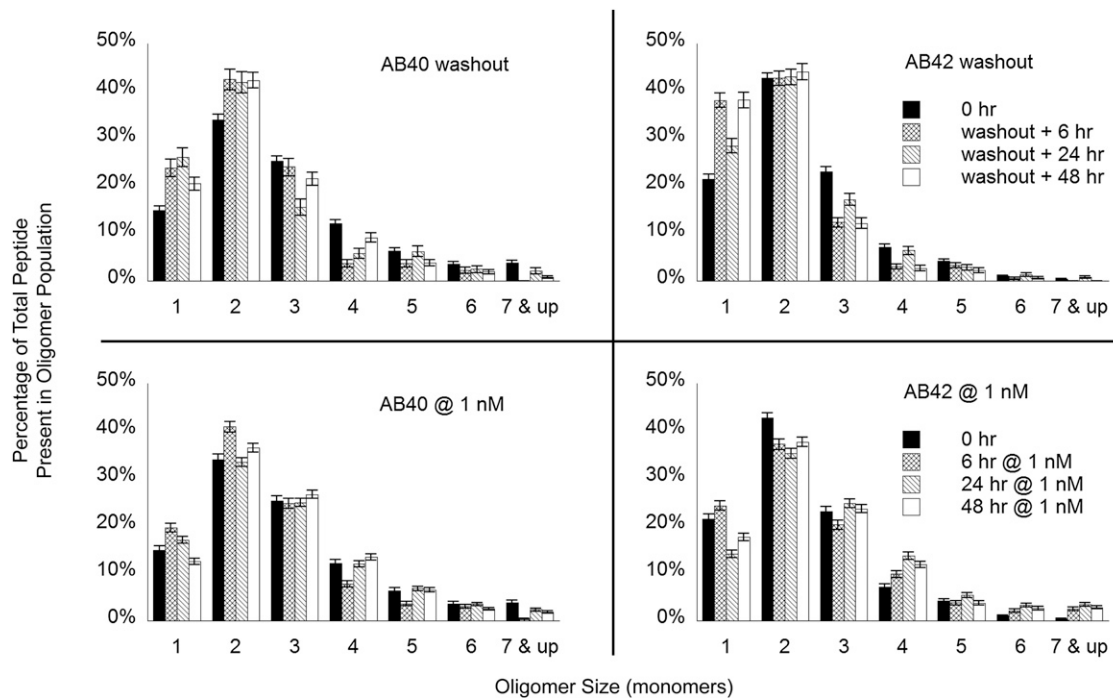
FIGURE 3 On-neurite oligomer size distribution depends on peptide identity and presence of solution peptide. As illustrated in Fig. S7, primary rat hippocampal cell cultures were treated with 1 nM HL647Aβ40 or 42 for 10 min, and then incubated a further 6, 24, or 48 h in media containing no Aβ (*washout plots*, shown at *left*), or containing 1 nM Aβ (*1 nM plots*, shown at *right*). Results are plotted as proportion of total peptide present as oligomers of each size. Percentages were calculated from totals from two separate experiments, 30 images per experiment. Each sample contains at least 450 peptide subunits present in a minimum of 250 oligomers (see the Supporting Material, for exact numbers). Error bars represent standard error of the percentage.

Material (Fig. S6). Overall, 60% to 70% of particles did not exhibit detectable motion over the course of 10 scans. This value is consistent with the proportion of cell-bound oligomers exhibiting highly confined motion (motion on a spatial and temporal scale that would not be detectable with 10 sequential xyt scans) observed in a recent single-particle tracking study of Aβ42 on SH-SY5Y cells (52% to 77%, depending on type of oligomer) (34).

Neurite-bound oligomer size dynamics depend on peptide identity and solution peptide content

To study the kinetics of neurite-bound oligomer growth and dissociation, we obtained oligomer size distributions at several time points during incubations with or without peptide in solution. Cultures were incubated with 1 nM HL647Aβ40 or HL647Aβ42 for 10 min and then further incubated for up to another 48 h in the presence or absence of HL647Aβ40 or HL647Aβ42 (Fig. S7). On-neurite oligomer size distributions were then plotted for each treatment condition. Example images from the 48 h time points are shown in Fig. S3.

Examination of these results reveals trends in the distribution of oligomer sizes over time. In particular, for HL647Aβ40, there is an observable increase in the proportion of total Aβ peptide present as monomer and dimer in samples incubated in the absence of peptide (*washout*

samples in top left plot, Fig. 3). For HL647Aβ42, this increase is restricted to monomers, and a decrease in the proportion of peptide present as trimers is also observed (*top right plot*, Fig. 3). For both peptides, the raw oligomer size distributions shift significantly toward smaller oligomers after 48 h incubation without peptide in solution, as compared to the distributions following initial exposure (Mann-Whitney U test, $p < 0.0005$ for Aβ40, $p < 0.00001$ for Aβ42). Average oligomer sizes changed from 2.2 to 1.9 peptide subunits for HL647Aβ40 and from 1.9 to 1.5 peptide subunits for HL647Aβ42. When neurites are continuously incubated with 1 nM HL647Aβ40, the size distribution exhibits no significant change over time (*bottom left plot*, Fig. 3). For neurites continuously exposed to 1 nM HL647Aβ42, very subtle decreases in the proportion of peptide present as monomer and dimer reflect increases in the proportion present in tetramers and hexamers and greater. Indeed, a small but significant shift toward larger oligomers is present in the Aβ42 raw oligomer size distribution after 48 h with 1 nM peptide as compared to at 0 h (immediately following initial exposure) (Mann-Whitney U test, $p < 0.005$). The average Aβ42 oligomer size changes from 1.9 to 2.0 peptide subunits. Of importance, raw numbers of monomers and dimers present on the neurites are not significantly decreased in either sample, following 6 to 48 h incubation at 1 nM (Fig. S5).

In recent years, interest in a potential synergy between Aβ42 and Aβ40 in oligomer formation and toxicity has increased, due to reports that AD development may depend sensitively on the ratio of the two peptides in the brain. Familial AD-associated mutations in presenilins 1 and 2 significantly increase the Aβ42:Aβ40 ratio in transfected cultured cells and transgenic mice (35–37), and a higher Aβ42:Aβ40 ratio is correlated with earlier age-of-onset in humans with these mutations (38,39). To determine whether membrane-bound Aβ oligomer evolution is affected by increases in Aβ42:Aβ40 ratio, we premixed HL647Aβ42 and HL647Aβ40 and performed single-molecule oligomer size measurements on neurite-bound oligomers formed from the mixture. As the exact Aβ42:Aβ40 ratio reported in the literature for FAD mutations varies widely, Aβ42 and Aβ40 were mixed at a 1:1 ratio.

Interestingly, comparison of raw oligomer size distributions reveals that neurite-bound oligomers detected after 10 min exposure to this mixture at 1 nM (shown in Fig. S3) were significantly smaller overall than those detected on neurites incubated with either peptide alone, with an average size of 1.6 peptide subunits (Mann-Whitney U-test, $p < 0.00001$ for both 1:1 Mix versus Aβ40 and 1:1 Mix versus Aβ42). For mixed on-neurite oligomers, 80% of the peptide shows up in the monomer-dimer populations (Fig. 4). In contrast, when present alone, only 50% and 66% of HL647Aβ40 and 42, respectively, are present as monomer-dimers (Fig. 2). This result is not unexpected, given that Aβ40 and Aβ42 have been shown to inhibit each other's oligomerization in solution, albeit at higher concentrations than used here (40). Perhaps more surprisingly, the raw oligomer size distribution of mixed oligomers observed on the slides (with an average oligomer size of 1.9 peptide subunits) is significantly shifted toward larger oligomers as compared to what is seen for either peptide alone (Mann-Whitney U-test, $p < 0.00001$). This may indicate that, conversely to the results obtained by Murray and colleagues at micromolar concentrations, the Aβ42:Aβ40 pair dimerizes and forms larger oligomers more easily than Aβ40:Aβ40 or Aβ42:Aβ42 at low nanomolar levels. Alternately, the interaction with the poly-D-lysine coated coverslip may facilitate oligomerization of the mixed peptide more so than it does for Aβ40 or Aβ42 individually.

To determine how mixing of the two peptides affects on-membrane oligomerization, neurites were treated with 1 nM of the 1:1 mix for 10 min, and oligomer size distributions were obtained after further incubations of 24 and 48 h, with and without the peptide in solution (Fig. 4). In contrast to the data with either peptide alone, in samples incubated following peptide washout the proportion of peptide present as monomers decreases by 24 to 48 h. This results in slight increases in the proportion of peptide subunits present as dimers, trimers, and tetramers. Comparison of the raw distributions reveals that on-membrane oligomers of the 1:1 mix grow significantly over 48 h as compared to the 0 h sample
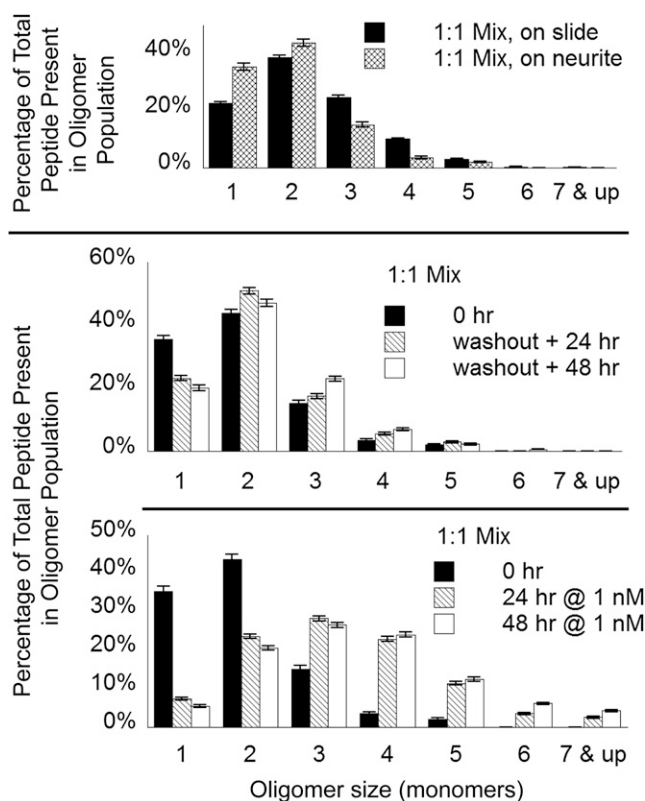

FIGURE 4 Oligomers formed from a 1:1 mix of Aβ40:Aβ42 exhibit more significant growth. Distributions are shown as percentage of total monomer present as oligomer of each size. The top plot represents size distributions for mixed oligomers nonspecifically bound to slides or bound to primary rat hippocampal neurites. Percentages were calculated from totals from three separate experiments for neurite-bound and two separate experiments for slide-bound oligomers, 15 to 20 images per experiment. Middle and bottom plots show evolution of oligomer size distributions over up to 48 h. Samples were treated as in Fig. 3. Percentages were calculated from totals from two separate experiments, 30 images per experiment. Each sample contains at least 1400 peptide subunits present in a minimum of 600 particles (see Supporting Material for exact numbers). Error bars represent standard error of the percentage.

even in the absence (or in the presence of exceedingly low concentrations) of solution peptide (Mann-Whitney U-test, $p < 0.00001$). Oligomers in the washout 1:1 mixed sample had an average size of 1.9 peptide subunits.

For neurites incubated in the continued presence of 1 nM 1:1 mixed Aβ42:Aβ40, a very substantial shift toward larger oligomers occurs within 24 to 48 h. The proportion of total peptide present as monomer decreases by roughly 30 percentage points within 24 h, and the proportion present as dimer decreases by 20 percentage points (bottom plot, Fig. 4). Interestingly, for the 1:1 mixed peptide, the drop in proportion of total peptide present as monomer is in part due to a drop in the raw number of monomers present on the neurites over time (Fig. S8). These large decreases in the proportion of peptide contained in small oligomers translate to large increases in the peptide present as trimers through heptamers and larger oligomers, with a significant

increase in size for the 48 h sample as compared to the 0 h sample (Mann-Whitney U-test, $p < 0.00001$). Average oligomer size shifts from the previously mentioned 1.6 peptide subunits to 2.9 peptide subunits. Mixture of the two peptides at a 1:1 ratio thus has a large impact on oligomer size on the neurite membrane, inducing greater growth over the hours to days following initial exposure.

The data presented thus far do not directly indicate that individual oligomers formed from the 1:1 mixed peptide contain both HL647Aβ42 and HL647Aβ40. However, this is the most plausible explanation for the strong effects of mixing on the on-membrane oligomerization kinetics observed here. Recent surface plasmon resonance experiments have indicated that Aβ40 and Aβ42 bind to each other, albeit more weakly than either peptide self-associates (41). In the same study, Aβ40 was shown to slow Aβ42 fibril formation, such that fibrillization proceeded at the same rate for both peptides in a 1:1 mix of the two. These results were interpreted as strong evidence for formation of mixed fibrils. Another group also recently showed that incubating Aβ40 at a 1:1 ratio with Aβ42 inhibits Aβ42 fibril formation, but the authors of the study explicitly state that formation of high-order prefibrillar structures is not slowed (42). To test whether combined Aβ40 and Aβ42 oligomer (mixed oligomer) formation can occur, we performed FRET (fluorescence resonance energy transfer) experiments using neurites treated with HL555Aβ40 and HL647Aβ42. To obtain sufficient signal, neurons were incubated with 2 nM HL555Aβ40 and 2 nM HL647Aβ42 for 10 min. We do observe FRET signal between the two peptides within neurite-bound oligomers (Fig. S9). Further exploration into the exact Aβ40:Aβ42 stoichiometry of such mixed oligomers is in progress (Chang, C., manuscript in preparation).

Total quantities of peptide bound over time depend on peptide identity

To form a scheme that is consistent with our observations, it is helpful to examine the total quantities of peptide bound to the neurites at each time point. Interestingly, the total quantity of peptide bound after a 10 min incubation at 1 nM is similar under all three conditions (Fig. 5). Following washout or at 1 nM Aβ incubation conditions, HL647Aβ40 and HL647Aβ42 total peptide follow similar trends: total neurite-bound peptide decreases over time when no peptide is present in solution and increases slightly on incubation with 1 nM Aβ. The 1:1 mix of the two peptides, however, shows a much larger increase in total peptide bound on incubation with 1 nM Aβ. This substantial increase in the total amount of peptide bound likely contributes strongly to the oligomer growth observed in the 1:1 samples at 1 nM over 48 h (Fig. 4, *lowest plot*).

Paradoxically, an increase in total peptide bound is also observed when no peptide is present in solution. This is most likely because, as shown in the example images in
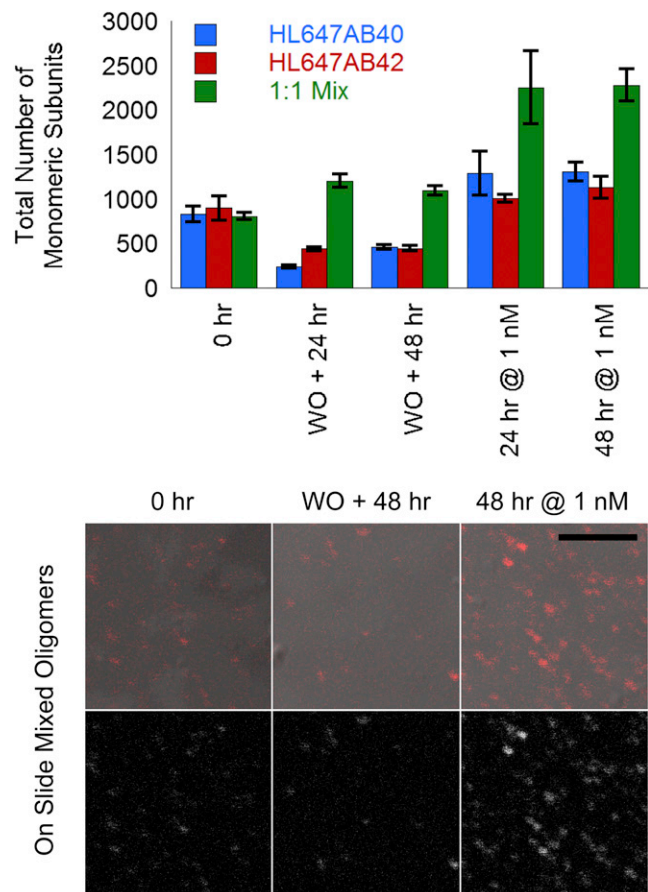

FIGURE 5   Total numbers of peptide subunits bound to neurites over time depend on peptide identity and presence of solution peptide. The upper plot depicts the raw number of monomeric subunits on neurites at 24 h and 48 h following an initial 10 min incubation. Bars labeled with WO represent washout samples incubated without peptide in the media; bars labeled @ 1 nM represent samples incubated with 1 nM peptide in the media. The images below illustrate the density of oligomers of a 1:1 mix on slides immediately after a 10 min incubation, at 48 h following peptide washout, and after 48 h in 1 nM peptide. Scale bar, 5 μm.

the lower section of Fig. 5, ~50% of the slide-bound 1:1 HL647Aβ40:42 oligomers are lost after 24 to 48 h incubation without peptide in solution. This peptide is then available for binding to the membrane and membrane bound oligomers. Similar decreases in slide-bound oligomer density are noted for both HL647Aβ40 and HL647Aβ42 alone, but the on-slide oligomer density is lower for each of these (20 $\pm$ 5 oligomers per frame for HL647Aβ40 and 44 $\pm$ 4 oligomers per frame for HL647Aβ42, versus 64 $\pm$ 2 oligomers per frame for the mixed peptide).

Assuming that half the slide-bound peptide dissociates into solution results in an estimated postwashout concentration of ~2 fM 1:1 HL647Aβ40:42. The binding affinity of the 1:1 mixed oligomers for the membrane would have to be extremely high for the neurites to bind additional peptide under these conditions. However, the 1:1 mixed oligomers appear to aggregate rapidly enough on the membrane to

reduce the overall number of neurite-bound monomers over time, possibly opening up monomer binding sites to solution peptide. Additionally, possibly due to their increased size, oligomers formed from 1:1 HL647Aβ40:42 may have unique effects on the neurite membrane composition which increase the Aβ-membrane affinity (enrichment in externalized phosphatidylserine, for instance).

DISCUSSION

Our previous work showed that Aβ40 dissolved in media or buffers containing physiological salts forms oligomers up to hexamers in size on glass surfaces from the mixture of monomers and dimers initially present in freshly solubilized peptide (27). In the current study, this result is reproduced with both Aβ40 and Aβ42 (Fig. S1 and Fig. 2, *black bars*). Mixed peptide forms smaller oligomers on neurites and larger ones on the slide, whereas either peptide alone forms larger neurite-bound oligomers than it forms on the slide. This result shows that oligomerization on glass surfaces in media or physiological buffer proceeds along a distinct pathway as compared to that on membranes. Although neurite membrane appears to accelerate the formation of larger oligomers (or selectively bind larger oligomers) for each peptide individually, it initially associates with smaller oligomers of the 1:1 mix. However, the total initial quantities of all three peptide combinations bound following 10 min incubation at 1 nM Aβ are equivalent within experimental error. A kinetic model can be proposed to explain these results. A possible schema for oligomers' interactions with membranes is shown in Fig. 6. Although this mechanism is likely oversimplified, it is nevertheless useful in interpreting our observations. Exact rate constants for these processes remain unknown, but the data presented here can be used to assemble a qualitative model in which the identity of the peptide controls the rate and quantity of binding. On the basis of our results, we hypothesize that monomers and dimers of the peptides may bind to the neurites at the same initial rate (k_{on}) but may have dissociation rates (k_{off}), oligomer growth rates (k_{olig}), and large oligomer clearance/dissociation rates (k_{deol}) dependent upon the peptide identity.

On-neurite oligomer growth may proceed very rapidly for Aβ40 (high k_{olig}), so that within minutes the neurite-bound oligomers reach stable sizes. This would explain why little growth occurs between initial exposure and the 48 h time point (Fig. 3, *lower left plot*). For Aβ42, growth may also proceed rapidly, but after the initial phase of rapid formation of larger oligomers, additional slow oligomer growth may continue (Fig. 3, *lower right plot*). The initial smaller size and the large degree of growth of the mixed oligomers over 48 h could be explained if formation of larger oligomers on the membrane were much slower for the mixed peptide than for either Aβ42 or Aβ40 alone (lower k_{olig}). In light of recent evidence that neuroblastoma cells can

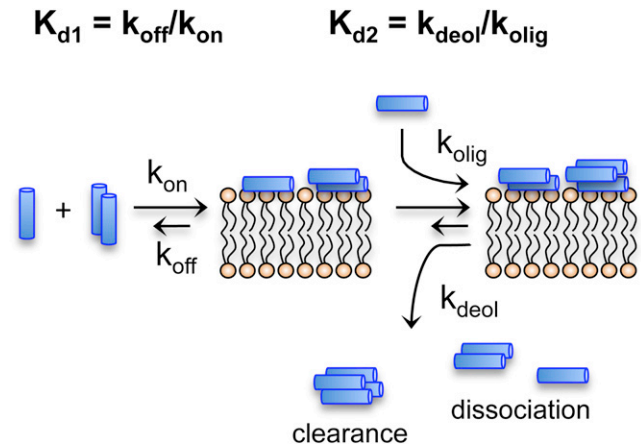$$K_{d1} = k_{off}/k_{on} \qquad K_{d2} = k_{deol}/k_{olig}$$

FIGURE 6 Binding and on-membrane oligomerization kinetics depend on peptide identity. A model is proposed to explain observed oligomer interactions with neurite membranes. K_{d1}, dissociation constant for initial binding to membrane; K_{d2}, dissociation constant for on-membrane oligomerization; k_{on}, rate constant for binding of small oligomers to membrane; k_{off}, rate constant for dissociation of small oligomers from membrane; k_{olig}, rate constant for on-membrane oligomerization; k_{deol}, rate constant for deoligomerization (a group of processes including dissociation of large oligomers into small ones, dissociation of oligomers from the membrane, and cellular clearance of membrane-bound oligomers). Small 1:1 mixed oligomers may bind more tightly to membranes than oligomers of either peptide alone and grow more slowly. However, once larger oligomers of the 1:1 mix form, they may be more stable (or less easily cleared by the cell) than oligomers of either peptide alone.

internalize single Aβ oligomers (34), the increased size observed for the mixed oligomers after 24 to 48 h may also indicate that the cell's ability to clear large mixed oligomers is reduced as compared to its ability to clear homogeneous aggregates of either peptide (lower k_{deol} for mixed peptide than for Aβ40 or Aβ42). Of importance, as FRET can be observed between Aβ40 and Aβ42 on neurites (Fig. S9), a substantial portion of oligomers in the mixed sample likely contain both peptides. These observations have important implications for AD. FAD-associated mutations in presenilins 1 and 2 significantly increase Aβ42:Aβ40 ratio in transfected cultured cells and transgenic mice (35–37), and higher Aβ42:Aβ40 ratio is correlated with earlier age-of-onset in humans with these mutations (38,39).

In a number of preliminary experiments, we did not observe grossly apparent toxicity in cells treated for up to 48 h with Aβ concentrations in the 1 to 10 nM range. Therefore, understanding the time evolution of the functional effects of these oligomers will require further study. Jan and colleagues (42) observed higher viability levels in rat cortical neurons treated with a 1:1 mix of initially monomeric Aβ40 and Aβ42 as compared with cells treated with equimolar amounts of either peptide alone. This study was, however, performed at 10 μM peptide (10,000 times the level used here) and did not assess subtle measures of neurophysiology. More recently, Kuperstein et al. (43)

treated neurons with 1 μM peptide for only 2 h and demonstrated that under these conditions, a 3:7 ratio of Aβ42/Aβ40 reduced the neuronal firing rate to a greater degree than Aβ42 alone. If oligomer neurotoxicity or modulation of synaptic function increase with oligomer size, as some have suggested (44,45), the current results might help explain the observations of Kuperstein and colleagues.

We did not observe initial binding of Aβ40 or Aβ42 at low nanomolar concentrations to be synaptically localized (Fig. S4), and on-neurite oligomers are only slightly more densely distributed on dendrites than on axons after a 10 min exposure (Fig. S5). A difference of the magnitude observed here could be due to differences in membrane composition or to higher density of Aβ receptor proteins on dendrites. Although a number of studies have reported that Aβ preferentially binds to synapses (18,30,31), these have all to our knowledge either used preaggregated oligomers or stained for endogenous oligomers in model mice using an antioligomer antibody. These studies may therefore have overlooked low-molecular weight oligomers formed in contact with the membrane, the behavior of which is the focus of the current work. The oligomers described here may represent precursor structures to preaggregated oligomers or a structurally distinct set of Aβ aggregates that can only form in contact with neuronal membranes. We note, however, that confocal mode kymographs (Fig. S6) identified a small portion of neurite-bound oligomers which are mobile (20% to 30%). Migration of these oligomers to cell membrane regions containing specific receptors or even to synapses could occur given sufficient time.

CONCLUSIONS

In the work presented here, a single-molecule microscopy method was applied to identify and characterize fluorescently labeled Aβ oligomers on the neurites of living cells and to follow their time evolution. The results point to a mechanism by which, at physiological concentrations, very small Aβ oligomers bind to the membrane and grow on the membrane over time, with kinetics dependent upon the local Aβ42:Aβ40 ratio. Such oligomers may gradually localize to synapses and interfere with function of specific membrane proteins or aggregate further to directly form toxic pores in biological membranes. Recent work in our laboratory has demonstrated that Aβ40 oligomers must contain at least six monomeric subunits to induce significant conductivity in model membranes (28). The quantities of such structures observed on the timescales examined here are minimal and probably result in only subtle changes to neuronal function. These results provide new, to our knowledge, insight into the dynamics and mechanism of Aβ binding and oligomer formation on membranes at physiological concentrations. They also provide a foundation for future studies into the time, concentration, and Aβ42:Aβ40 ratio dependence of oligomer growth and the correlation of these factors with neurotoxicity.

SUPPORTING MATERIAL

REFERENCES

1. Alzheimer's Association. 2012. 2012 Alzheimer's disease facts and figures. *Alzheimers Dement.* 8:131–168.

2. Klein, W. L. 2002. Abeta toxicity in Alzheimer's disease: globular oligomers (ADDLs) as new vaccine and drug targets. *Neurochem. Int.* 41:345–352.

3. Crouch, P. J., S.-M. E. Harding, …, C. L. Masters. 2008. Mechanisms of A β mediated neurodegeneration in Alzheimer's disease. *Int. J. Biochem. Cell Biol.* 40:181–198.

4. Yu, J.-T., R. C.-C. Chang, and L. Tan. 2009. Calcium dysregulation in Alzheimer's disease: from mechanisms to therapeutic opportunities. *Prog. Neurobiol.* 89:240–255.

5. McLean, C. A., R. A. Cherny, …, C. L. Masters. 1999. Soluble pool of Abeta amyloid as a determinant of severity of neurodegeneration in Alzheimer's disease. *Ann. Neurol.* 46:860–866.

6. Lue, L. F., Y. M. Kuo, …, J. Rogers. 1999. Soluble amyloid β peptide concentration as a predictor of synaptic change in Alzheimer's disease. *Am. J. Pathol.* 155:853–862.

7. Bitan, G., M. D. Kirkitadze, …, D. B. Teplow. 2003. Amyloid β-protein (Abeta) assembly: Abeta 40 and Abeta 42 oligomerize through distinct pathways. *Proc. Natl. Acad. Sci. USA.* 100:330–335.

8. Bitan, G., A. Lomakin, and D. B. Teplow. 2001. Amyloid β-protein oligomerization: prenucleation interactions revealed by photo-induced cross-linking of unmodified proteins. *J. Biol. Chem.* 276:35176–35184.

9. Ding, H., P. T. Wong, …, D. G. Steel. 2009. Determination of the oligomer size of amyloidogenic protein β-amyloid(1-40) by single-molecule spectroscopy. *Biophys. J.* 97:912–921.

10. Lee, G., H. B. Pollard, and N. Arispe. 2002. Annexin 5 and apolipoprotein E2 protect against Alzheimer's amyloid-β-peptide cytotoxicity by competitive inhibition at a common phosphatidylserine interaction site. *Peptides.* 23:1249–1263.

11. Simakova, O., and N. J. Arispe. 2007. The cell-selective neurotoxicity of the Alzheimer's Abeta peptide is determined by surface phosphatidylserine and cytosolic ATP levels. Membrane binding is required for Abeta toxicity. *J. Neurosci.* 27:13719–13729.

12. Williamson, R., A. Usardi, …, B. H. Anderton. 2008. Membrane-bound β-amyloid oligomers are recruited into lipid rafts by a fyn-dependent mechanism. *FASEB J.* 22:1552–1559.

13. Zampagni, M., E. Evangelisti, …, C. Cecchi. 2010. Lipid rafts are primary mediators of amyloid oxidative attack on plasma membrane. *J. Mol. Med.* 88:597–608.

14. Nicholson, A. M., and A. Ferreira. 2009. Increased membrane cholesterol might render mature hippocampal neurons more susceptible to

β-amyloid-induced calpain activation and tau toxicity. *J. Neurosci.* 29:4640–4651.

15. Bateman, D. A., J. McLaurin, and A. Chakrabartty. 2007. Requirement of aggregation propensity of Alzheimer amyloid peptides for neuronal cell surface binding. *BMC Neurosci.* 8:29.

16. Wang, H. Y., D. H. Lee, …, A. B. Reitz. 2000. β-Amyloid(1-42) binds to α7 nicotinic acetylcholine receptor with high affinity. Implications for Alzheimer's disease pathology. *J. Biol. Chem.* 275:5626–5632.

17. Laurén, J., D. A. Gimbel, …, S. M. Strittmatter. 2009. Cellular prion protein mediates impairment of synaptic plasticity by amyloid-β oligomers. *Nature.* 457:1128–1132.

18. Renner, M., P. N. Lacor, …, A. Triller. 2010. Deleterious effects of amyloid β oligomers acting as an extracellular scaffold for mGluR5. *Neuron.* 66:739–754.

19. Cissé, M., B. Halabisky, …, L. Mucke. 2011. Reversing EphB2 depletion rescues cognitive functions in Alzheimer model. *Nature.* 469:47–52.

20. Benilova, I., E. Karran, and B. De Strooper. 2012. The toxic Aβ oligomer and Alzheimer's disease: an emperor in need of clothes. *Nat. Neurosci.* 15:349–357.

21. Dahlgren, K. N., A. M. Manelli, …, M. J. LaDu. 2002. Oligomeric and fibrillar species of amyloid-β peptides differentially affect neuronal viability. *J. Biol. Chem.* 277:32046–32053.

22. Demuro, A., E. Mina, …, C. G. Glabe. 2005. Calcium dysregulation and membrane disruption as a ubiquitous neurotoxic mechanism of soluble amyloid oligomers. *J. Biol. Chem.* 280:17294–17300.

23. Arispe, N., H. B. Pollard, and E. Rojas. 1993. Giant multilevel cation channels formed by Alzheimer disease amyloid beta-protein [A beta P-(1-40)] in bilayer membranes. *Proc. Natl. Acad. Sci. USA.* 90:10573–10577.

24. Kawahara, M., N. Arispe, …, E. Rojas. 1997. Alzheimer's disease amyloid β-protein forms Zn(2+)-sensitive, cation-selective channels across excised membrane patches from hypothalamic neurons. *Biophys. J.* 73:67–75.

25. Zhang, Y.-J., J.-M. Shi, …, S. R. Ji. 2012. Intra-membrane oligomerization and extra-membrane oligomerization of amyloid-β peptide are competing processes as a result of distinct patterns of motif interplay. *J. Biol. Chem.* 287:748–756.

26. Shankar, G. M., S. Li, …, D. J. Selkoe. 2008. Amyloid-β protein dimers isolated directly from Alzheimer's brains impair synaptic plasticity and memory. *Nat. Med.* 14:837–842.

27. Johnson, R. D., J. A. Schauerte, …, D. G. Steel. 2011. Direct observation of single amyloid-β(1-40) oligomers on live cells: binding and growth at physiological concentrations. *PLoS ONE.* 6:e23970.

28. Schauerte, J. A., P. T. Wong, …, A. Gafni. 2010. Simultaneous single-molecule fluorescence and conductivity studies reveal distinct classes of Abeta species on lipid bilayers. *Biochemistry.* 49:3031–3039.

29. Jakawich, S. K., H. B. Nasser, …, M. A. Sutton. 2010. Local presynaptic activity gates homeostatic changes in presynaptic function driven by dendritic BDNF synthesis. *Neuron.* 68:1143–1158.

30. Lacor, P. N., M. C. Buniel, …, W. L. Klein. 2004. Synaptic targeting by Alzheimer's-related amyloid β oligomers. *J. Neurosci.* 24:10191–10200.

31. Koffie, R. M., M. Meyer-Luehmann, …, T. L. Spires-Jones. 2009. Oligomeric amyloid beta associates with postsynaptic densities and correlates with excitatory synapse loss near senile plaques. *Proc. Natl. Acad. Sci. USA.* 106:4012–4017.

32. Mitrano, D. A., and Y. Smith. 2007. Comparative analysis of the subcellular and subsynaptic localization of mGluR1a and mGluR5 metabotropic glutamate receptors in the shell and core of the nucleus accumbens in rat and monkey. *J. Comp. Neurol.* 500:788–806.

33. Hardingham, G. E., and H. Bading. 2010. Synaptic versus extrasynaptic NMDA receptor signalling: implications for neurodegenerative disorders. *Nat. Rev. Neurosci.* 11:682–696.

34. Calamai, M., and F. S. Pavone. 2011. Single molecule tracking analysis reveals that the surface mobility of amyloid oligomers is driven by their conformational structure. *J. Am. Chem. Soc.* 133:12001–12008.

35. Duff, K., C. Eckman, …, S. Younkin. 1996. Increased amyloid-β42(43) in brains of mice expressing mutant presenilin 1. *Nature.* 383:710–713.

36. Citron, M., D. Westaway, …, D. J. Selkoe. 1997. Mutant presenilins of Alzheimer's disease increase production of 42-residue amyloid β-protein in both transfected cells and transgenic mice. *Nat. Med.* 3:67–72.

37. Borchelt, D. R., G. Thinakaran, …, S. S. Sisodia. 1996. Familial Alzheimer's disease-linked presenilin 1 variants elevate Abeta1-42/1-40 ratio in vitro and in vivo. *Neuron.* 17:1005–1013.

38. Kumar-Singh, S., J. Theuns, …, C. Van Broeckhoven. 2006. Mean age-of-onset of familial alzheimer disease caused by presenilin mutations correlates with both increased Abeta42 and decreased Abeta40. *Hum. Mutat.* 27:686–695.

39. Walker, E. S., M. Martinez, …, A. Goate. 2005. Presenilin 2 familial Alzheimer's disease mutations result in partial loss of function and dramatic changes in Abeta 42/40 ratios. *J. Neurochem.* 92:294–301.

40. Murray, M., S. Bernstein, …, M. T. Bowers. 2009. Amyloid β protein : Aβ40 inhibits Aβ42 oligomerization. *J. Am. Chem. Soc.* 313:6316–6317.

41. Pauwels, K., T. L. Williams, …, K. Broersen. 2012. Structural basis for increased toxicity of pathological aβ42:aβ40 ratios in Alzheimer disease. *J. Biol. Chem.* 287:5650–5660.

42. Jan, A., O. Gokce, …, H. A. Lashuel. 2008. The ratio of monomeric to aggregated forms of Abeta40 and Abeta42 is an important determinant of amyloid-β aggregation, fibrillogenesis, and toxicity. *J. Biol. Chem.* 283:28176–28189.

43. Kuperstein, I., K. Broersen, …, B. De Strooper. 2010. Neurotoxicity of Alzheimer's disease Aβ peptides is induced by small changes in the Aβ42 to Aβ40 ratio. *EMBO J.* 29:3408–3420.

44. Ono, K., M. M. Condron, and D. B. Teplow. 2009. Structure-neurotoxicity relationships of amyloid β-protein oligomers. *Proc. Natl. Acad. Sci. USA.* 106:14745–14750.

45. O'Nuallain, B., D. B. Freir, …, D. M. Walsh. 2010. Amyloid β-protein dimers rapidly form stable synaptotoxic protofibrils. *J. Neurosci.* 30:14411–14419.